Journal of Hydrology 609 (2022) 127756

Contents lists available at ScienceDirect

Journal of Hydrology

journal homepage: www.elsevier.com/locate/jhydrol

Research papers

Suspended sediment transport and deposition in sediment-replenished artificial floods in Mediterranean rivers

Teresa Serra *, Marianna Soler, Aina Barcelona, Jordi Colomer

Department of Physics, Universitat de Girona, C/ de la Universitat de Girona, 4, 17003 Girona, Spain

ARTICLE INFO

This manuscript was handled by Marco Borga, Editor-in-Chief, with the assistance of Lorenzo Marchi, Associate Editor

Keywords:
Sediment transport
Sediment-replenishment
River restoration
Artificial water flood

ABSTRACT

Dams and impoundments constructed in rivers produce changes in their hydrological and sediment transport regimes, regulate their flows and reduce the supply of sediments downstream. Artificially inducing floods from reservoirs in conjunction with sediment-replenishment strategies is currently being employed to enhance sediment supply to river catchment areas. In this study, sediment-replenished artificial floods are compared to their non-sediment replenishment counterparts. The hysteretic loops between suspended sediment concentration and water flow present low normalized hysteresis indices (close to zero) in the sediment-replenished artificial flood events. In the current work, sediment-replenishment produced a balanced suspended sediment transport in contrast to the without sediment-replenishment cases. The normalized hysteresis indices varied between the different particle sizes studied and the same water flow, indicating that different types of particles are transported differently despite being in the same water flow. Furthermore, both the suspended sediment transport and the sedimentation rate of particles during the flood events was greater for the sediment replenishment cases than for the non-sediment-replenishment cases. All things considered, sediment-replenished artificial flooding provides a successful management strategy for a more balanced suspended sediment transport that could be used as a river restoration practice.

1. Introduction

Dams are infrastructures that store water to guarantee consumer water requirements, and to produce energy by regulating the water flow along a river. Although dams and impoundments have existed for thousands of years, the largest have been built in the last 60 years and account for a total of 58,000 dams worldwide (Mulligan et al., 2020). Besides these large dams, there are an estimated 16 million smaller impoundments more (Lehner et al., 2011). Dams and impoundments regulate river flow in such a way that they reduce flooding events and sediment transport (Zhang et al., 2020). Suspended sediment plays a crucial role in creating ecological habitats and transporting nutrients (Vercruysse et al., 2017). The resulting shortfall in the supply of river sediments modifies the substrate many species require for nesting and sheltering (Baisre and Arboleya, 2006). Furthermore, the accumulation of sediments upstream from the dam reduces the storage capacity of the reservoir, while downstream the lack of sediments causes bed erosion, reduces morphology diversity and produces a loss of connectivity with different nearby areas, especially in drought periods. The presence of a dam also produces downriver phytoplankton homogenization, thus compromising the ecosystem processes driven by the different phytoplankton communities (de Castro et al., 2021). Following the construction of a dam, the pre-dam riverbed sediment composition is transformed and different management strategies must then be employed to maintain the ecological biodiversity in the river. Such management methodologies attempt to mimic the natural flow regime of the river (Poff et al., 1997) to obtain full flow restoration. Since the flow of water is the crucial element that maintains the river's habitats, artificial flooding needs to be investigated to pinpoint the best strategies for restoring rivers (García de Jalón et al., 2017). Controlled flushing flows, for instance, can be applied (Kondolf and Wilcock, 1996) in regulated rivers. These flows are designed to empty water reservoirs and mimic the action of natural floods and are used in river restoration programs. However, in alpine water intakes for hydropower, flushing flows have been found to negatively impact downstream macroinvertebrate diversity (Gabbud et al., 2019). In such cases, the considerable increase in water turbidity, the high frequency of flushing events and the sudden decrease in water temperature of such water releases are

* Corresponding author.
E-mail address: teresa.serra@udg.edu (T. Serra).

https://doi.org/10.1016/j.jhydrol.2022.127756
Received 13 December 2021; Received in revised form 8 March 2022; Accepted 18 March 2022
Available online 22 March 2022

attributed to being the main causes of the negative impact on the ecosystem. Gabbud and Lane (2016) stated that the target of any intervention should be to reproduce the natural flow regime of the system and mimic what the natural system would have looked like before human intervention and its resulting impact. Therefore, before any strategies can be put into place, management objectives such as removing sand from pools, mobilizing fine sediment from the riverbed, eroding channel banks, or allowing sediment to be deposited onto the floodplains, must be specified. Likewise, any incompatibilities must also be identified. For example, the erosion of channel banks may imply mobilizing gravel from the riverbed, which might not be desirable, or a large flushing flood may also cause a loss of water and energy production. Besides this, sediment transport in rivers is a crucial mechanism in determining the transport of associated chemicals (Rodríguez-Blanco et al., 2018). In fact, the Water Framework Directive (EC, 2000) has identified hydrological regimes and sediment transport as being critical factors in guaranteeing integrated river management.

Restoring altered natural flow patterns in rivers is an ongoing issue for water managers. In this case, the main purpose of river restoration is to maintain the abundance of river species, chemicals and water sediments, and favour the connectivity between different river habitats and sections. In Spain, legislation requires compulsory artificial floods in some highly regulated water bodies. These flood events are released from the largest hydrological infrastructures situated in regions that do not suffer from water scarcity and provided that water requirements for human consumption can be fulfilled. The legislation also establishes the maximum water flow, its duration, and the temporal rate of the change (Agència Catalana de l'Aigua (ACA), 2005), with characteristic water floods varying for each watershed (Magdaleno, 2017).

Sediment particles are transported downstream of a river (Wohl et al., 2015) as suspended sediment (fine particles such as clays, silts, and fine sands) or bedload sediments (coarse particles such as gravels and coarse sands) (Vercruysse et al., 2017). Suspended sediments are dominant in river transport systems, representing 70% of the annual sediment reaching coastal areas (Vercruysse et al., 2017). Sediment-replenishment during flushing floods is a technique used to recreate natural sediment transport. This practice uses the supply of sediments that has been retained upstream from a dam and, thus, lacking in the river reaches. Sediment-replenishment has been also studied in the laboratory to investigate the in-channel bed stockpile method (Battisacco et al., 2016). Battisacco et al. (2016) found that complete submersion of the replenishment volume results in complete erosion of the placed sediment. Stähly et al. (2020) found that sediment-replenishment in flushing floods enhanced the transport of bedload sediment, and improved river habitats and the morphological diversity in the river downstream from a dam. In their study, they indicated the need to perform sediment-replenishment practices as close to a dam as possible to optimise sediment transport. When comparing the region of a river upstream of a reservoir to the region downstream from it, sediment-replenishment has been found to reduce the negative effect of damming by partially restoring species diversity (Katano et al., 2021) in the same way as river tributaries do. A multi-deposit sediment-replenishment technique using low water flows has also been tested and found suitable for increasing bedload sediment transport downstream due to the reduction in the river section at the replenishment area (Kantoush et al., 2010; Stähly et al., 2020; Ock et al., 2013). Consecutive sediment-replenishment on a laboratory scale set-up produced a lower sediment deposition in the second replenishment compared to the first (Bösch et al., 2016), however, consecutive sediment-replenishment has been found to increase the length of river restoration projects (Bösch et al., 2016). The effect of other restoration activities, for instance opening a check-dam, or removing the dam altogether, have also been studied. In the case of opening a check-dam drain outlet, the sediment supply produces a downstream decrease in net-spinning species and an increase in the prevalence of swimmers, indicating the restoration of the macroinvertebrate community (Itsukushima et al., 2019). Dam removal is also a river restoration tool option (Burroughs et al., 2009). For example, upon removing the Stronach Dam from Pine River (Wisconsin, USA), an increase in the river's flow velocity, lateral erosion and substrate coarsening was described (Burroughs et al., 2019). Nevertheless, ten years on from the dam's removal only 12% of the sediment retained in the impoundment has so far been mobilized, indicating that river rehabilitation might take years to decades to be completed (Burroughs et al., 2009).

The response of sediment to the water flow is usually non-linear and follows complex patterns that allow the process to be classified into different types (Williams, 1989). Hysteresis loops to further the understanding of sediment transport have been used in different studies (Katano et al., 2021; Pokrovsky and Schott, 2002). From the hysteresis curves, water floods can be classified into six different types: clockwise, anticlockwise, eight-shaped, single line plus one loop - either clockwise or anticlockwise, and single line plus two loops (Williams, 1989; Megnounif et al., 2013, Hamshaw et al., 2018). Specifically, and for the purpose of the present study, clockwise c-Q loops hold when the c/Q ratio is higher at the rising limb of the flood than during the falling limb and are associated to a sediment depletion in the catchment during the flood. There is a steep increase of c with Q during the rising limb, which is attributed to the rapid erosion of the riverbed. In the case of eight-shaped loops, hysteresis holds when there is a contribution sequence of different sediment sources, i.e., during the falling limb of the hydrograph new sediment sources connect late to the main channel resulting in a new sediment supply. Likewise, hysteresis loops have also helped to determine sediment sources and pathways during storm events in agricultural basins (Sherriff et al., 2016). The presence of agricultural areas with bare soils has been found to favour the transport of suspended sediment downstream during flooding events in Mediterranean intermittent rivers (Fortesa et al., 2021), with anticlockwise hysteretic loops being prevalent. In the small catchment of the Búger River, floods usually produce clockwise loops, indicating fine sediment depletion in the river catchment (Fortesa et al., 2021). Hysteretic loops have also been applied to the transport of DOC and nitrates in river catchments (Vaughan et al., 2017). DOC hysteresis was similar between DOC sources and hydrologic pathways, i.e., the delivery of nitrates to streams depended on land use and land cover between watersheds (Vaughan et al., 2017). Some authors have used the normalized sediment hysteresis loops to compare watersheds (Haddadchi and Hicks, 2021; Cao et al., 2021; Fortesa et al., 2021).

Although some studies have analysed the ecological impact of sediment-replenishment in some rivers, there is still a lack of knowledge concerning the characterization of the transport of sediment particles downstream, as well as the characterization of the flood though hysteresis cycles which has not been compared with or without sediment-replenishment for the different types of particles. The purpose of the present study is to fill these gaps of knowledge for different rivers situated in the western part of the Mediterranean area. The current study will focus on the transport of suspended sediment (SS) particles (i.e., fine sediment particles) in sediment-replenishment strategies carried out in rivers in the Mediterranean area and compare them to the case of floods non-sediment-replenishment. Since the role SS transport plays in the biodiversity, and the ecosystem functions and services of a river are still somewhat unknown, this current study attempts to gain further insight into SS transport in watersheds and its significance for river basin management.

2. Materials and Methods

2.1. Sites description

Three rivers were considered in this study: Llobregat, Ter and Muga, all of which are situated in Catalonia (NE Spain, Fig. 1a), originate in the eastern Pyrenees and discharge into the Mediterranean Sea. The Llobregat and Ter rivers, two of the major rivers in the Catalan inner river

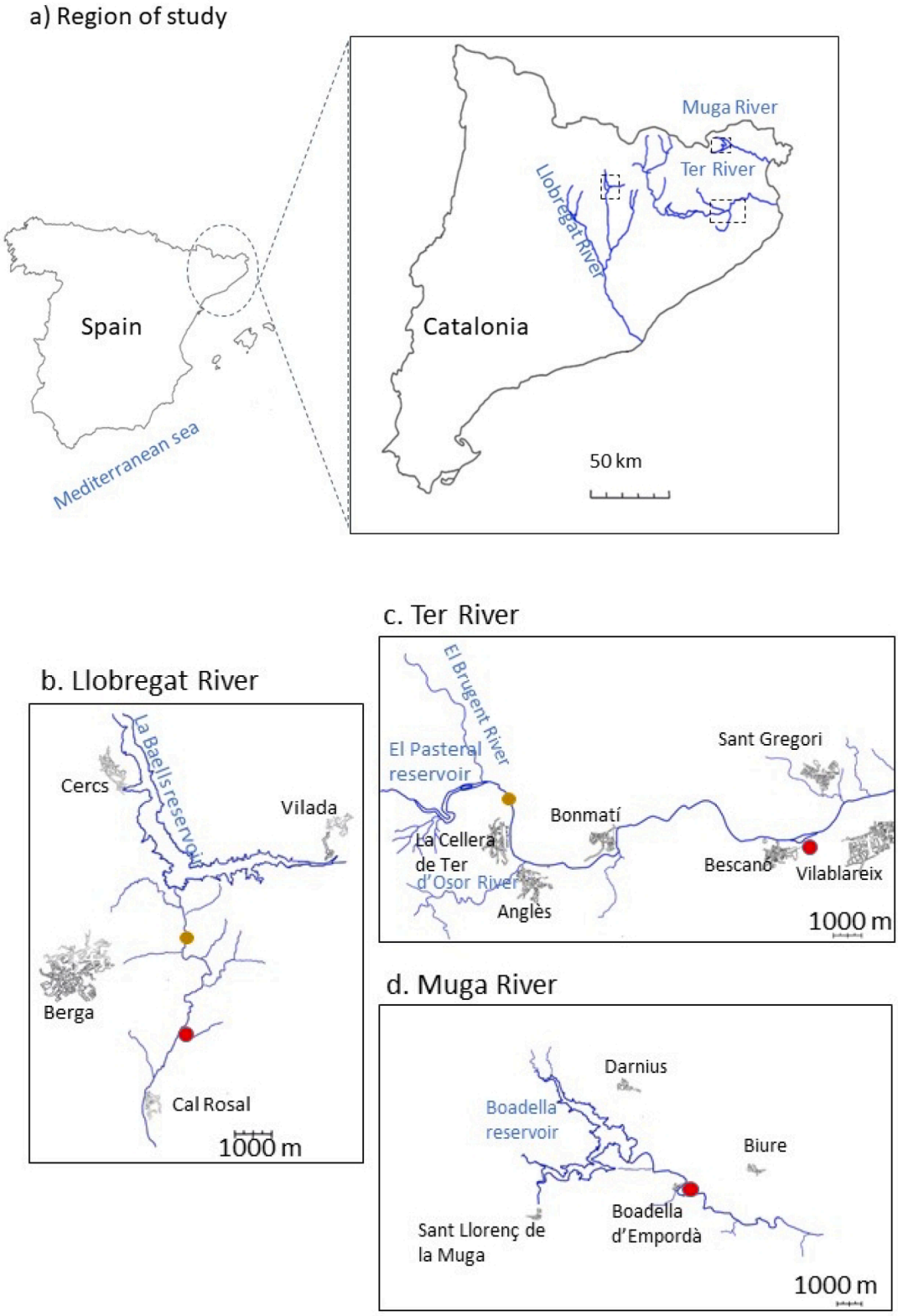

Fig. 1. a) Maps of Spain and Catalonia with the location of the three rivers under study (Ter, Muga and Llobregat). The dashed squares represent the areas shown in Fig. 1b-d. b) Map with the river course for the Llobregat, c) river course for the Ter and d) river course for the Muga. The upstream reservoirs have been included on the map and the towns closest to the rivers are also indicated. Effluent rivers have been included in cases where applicable. Red dots indicate the measurement position on each river for the present study. Brown dots indicate the position where sediment-replenishment was carried out in the cases where it was performed (Llobregat 2019 and Ter 2020 surveys). (For interpretation of the references to colour in this figure legend, the reader is referred to the web version of this article.)

basins, are the main water suppliers to the Barcelona and Girona-Costa Brava populations.

The Llobregat is 170 km long, has a catchment area of 4,948.3 km^2, and a mean annual water flow of 21.97 $m^3\ s^{-1}$ in its lower reaches. The Cal Rosal sampling point is situated at the beginning of the Llobregat's middle reach near the town of Berga (Fig. 1b), downstream from the La Baells dam which has a maximum capacity of 109.43 hm^3. In this reach, the Llobregat has a single channel in a V-Shaped valley that progressively opens downstream to a larger plain. The river flows over a rocky streambed with boulders and occasional gravel and sand bars, and its slope is 0.531%. The flow regime is controlled by the La Baells dam and at this point it has a mean annual flow of 7.01 $m^3\ s^{-1}$.

The river Ter is 208 km long, has a catchment area of 3,010 km^2, and a mean annual flow of 26.79 $m^3 s^{-1}$ in its lowest reach. Its discharge is highly dependent on the diversion regime which directs it towards the Barcelona and Girona metropolitan areas controlled by the Sau, Susqueda and El Pasteral reservoirs. These three dams are in the river's middle reach and upstream from the sampling point located at La Pilastra, near the village of Bescanó. The river's mean annual flow at the sampling site is of 21.43 $m^3\ s^{-1}$ and, like the Llobregat, is also controlled by the dam system management regimes (Fig. 1c). At La Pilastra, the stream flows over a terrace of alluvial sediments (mainly boulders, gravels, and sand), which forms an unconfined aquifer 10–12 m thick. The stream's mean slope is 0.088%. Several tributaries along the Ter's lowest region produce floods in periods of high rainfall, especially during spring and autumn. As mentioned above, three dams are situated upstream from the measurement point: the Sau, the Susqueda and El Pasteral reservoirs; the latter being situated near the town La Cellera de Ter (Fig. 2b). The Sau reservoir has a maximum capacity of 177 hm^3, the Susqueda 233 hm^3 and the El Pasteral reservoir 2 hm^3 (Fig. 1b). Downstream from the measuring point, there are two more small reservoirs (Resclosa de Colomers and Seva) with maximum capacities of 1 hm^3 and 1.1 hm^3, respectively.

The Muga River (Fig. 1d) provides water to the Figueres area and the north of the Costa Brava. It is 58 km long, has a catchment area of 853.8 km^2 and a mean water flow of 3.34 $m^3 s^{-1}$. However, it has a strong seasonal behaviour controlled by the lower summer rainfall rate and dam regulation, and also suffers from groundwater exploitation in its lower reach. Consequently, the Muga River discharge is highly impaired during the summer months. The Boadella reservoir, with a maximum capacity of 60.2 hm^3, was constructed on the Muga near the town Darnius (Fig. 1b). Although the mean annual discharge at the Boadella d'Empordà is 2.06 $m^3 s^{-1}$ this can vary greatly throughout the year. The Muga River near Boadella flows over sedimentary rock, both limestone and detritic lithologies, and locally it forms discontinuous terraces along its course of an approximate mean width of 250 m and expected thickness of<10 m. Its mean slope in the sampling reach is 0.303%.

The measuring points for the Llobregat and Muga rivers were located at the gauging stations downstream from the discharge, where a sediment trap was fixed to a wall found at the side of the river channel. The reported flow data correspond to the Catalan Water Agency gauging stations at these points. In the case of the Ter River, there is no gauging

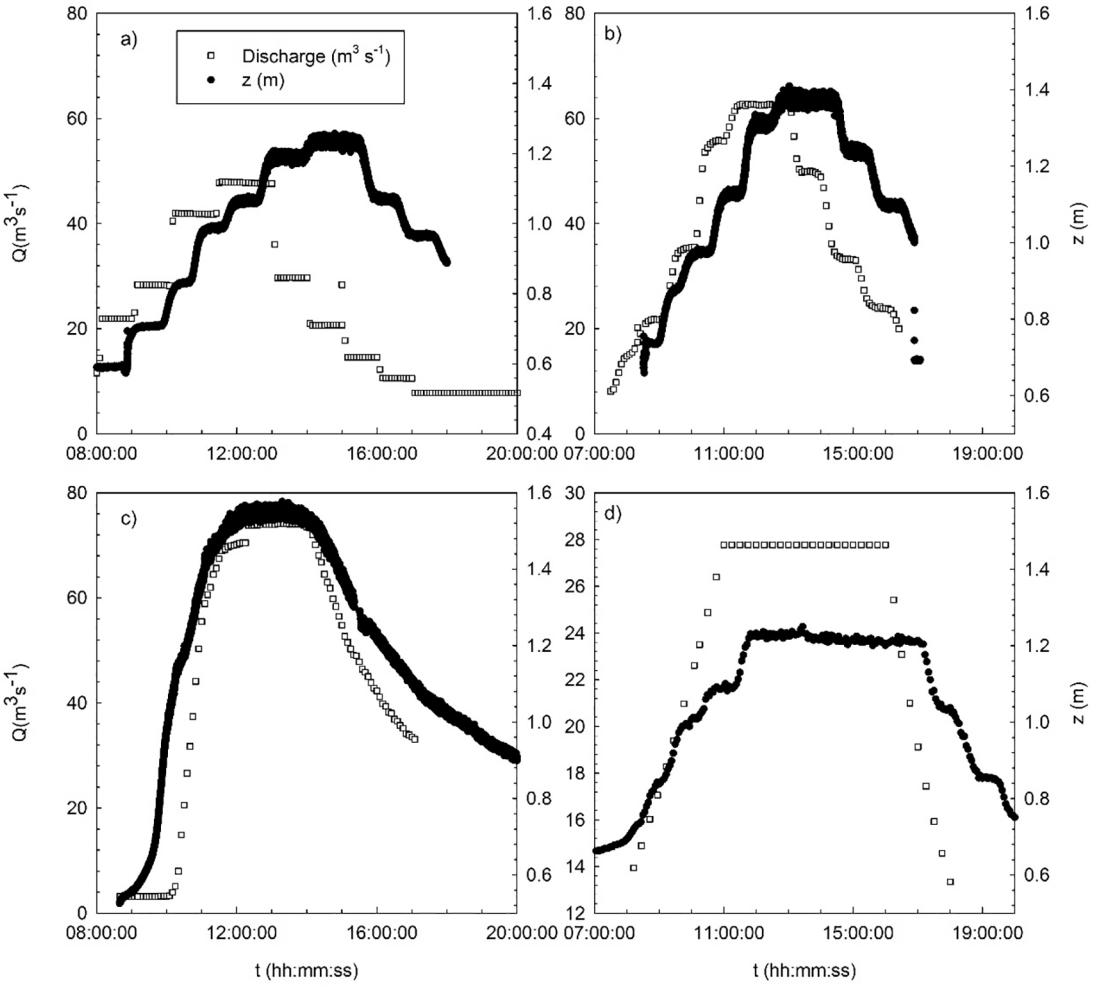

Fig. 2. Temporal evolution for the river flood in the four surveys carried out: Llobregat 2019 a), Llobregat 2020b), Ter 2020c) and Muga 2021 d). The water level (z, in m), measured with a thermistor (Seabird 37) at the study point for each survey, has also been plotted in each case.

station downstream from the discharge point and so flow data are from the nearest station located a few kilometres downstream. Consequently, the measuring point was situated near the town Bescanó (Fig. 1b), where the sediment trap was able to be fixed to an artificial wall usually used for sporting activities (La Pilastra site).

2.2. Artificial flooding

The water flood hydrograph followed the legislative regulations (Agència Catalana de l'Aigua (ACA), 2005). The maximum flood is obtained for each watershed as the mode of the flood distribution frequencies during the sixty-year period 1940–2000. The flood must be performed a minimum of once a year and when floods would naturally occur in the region. In the rising limb of the flood, the maximum rate of change of the flood between time steps is 1.8 times the flow rate, and the timestep is one hour. In contrast, in the falling limb of the flood the minimum rate of change is 0.7 times the flow rate, with the same timestep of one hour (Agència Catalana de l'Aigua (ACA), 2005).

The floods were performed during the experimental periods and with hydrographs following the regulations established by legislation for each watershed (Agència Catalana de l'Aigua (ACA), 2005). The Muga River had the lowest peak flow, in accordance with this river's smallest catchment area. Similar artificial floods were carried out in both the Llobregat and Ter rivers, with their larger catchment areas, with the Ter presenting the highest peak flow. The artificial water floods were carried out with and without sediment-replenishment in the Llobregat, with sediment-replenishment in the Ter, and without sediment-replenishment in the Muga. All floods had a rising limb, a plateau, and a falling limb (Fig. 2). In the Llobregat 2019 survey, the flood presented a gradual increase in the rising limb with a short plateau at the maximum flow (Fig. 2a). The maximum flow (51.34 $m^3\ s^{-1}$) was sustained for two hours and then started to decrease gradually. In the Llobregat 2020 survey, the rising limb of the flood was the steepest, and the maximum flow was also sustained for two hours and then started to decrease in the falling limb (Fig. 2b). The maximum flow in this survey was 62.92 $m^3\ s^{-1}$ (Fig. 2b), 1.2 times that in the Llobregat 2019 survey (Fig. 2a). In the Ter 2020 survey, the flood presented the steepest rising limb and the highest flow of the three surveys carried out (Fig. 2c). The maximum flow of 74.12 $m^3\ s^{-1}$ was sustained for three hours, after which it started to gradually decrease in the falling limb (Fig. 2c). The flood in the Muga River was the smallest in terms of the maximum flow rate: 27.70 $m^3\ s^{-1}$ (Fig. 2d). The rising limb was gradual, and the maximum flood was sustained for four hours, after which it started to gradually decrease in the falling limb (Fig. 2d). At the measuring point, the water level was measured with a pressure sensor and had a pattern similar to that of the temporal evolution of the flood. In all the cases, except for the Ter River, the flow was measured upstream from the sampling point. Therefore, the temporal evolution of the water level did not match with the temporal evolution of the water level at the measuring station. For the Ter, the flow was measured at the Girona station close to the study site. Thus, in this case, the evolution of the water flood and the water level transpired nearly at the same time (Fig. 2c). Therefore, in the current study, the evolution of the water level at the sampling point will be used as a proxy for the flow (Q) to plot the hysteresis loops c-z diagrams at each location (instead of using c-Q, given that we do not have the measurements of Q at the same measuring point as c). More details of the flooding event performed in each river are given in Table 1.

2.3. Methods for the suspended sediment measurements

To measure the suspended particle concentrations, 100 mL water samples were collected every fifteen minutes at the measuring position on each river for the length of the flood. Forty samples were collected in both the Llobregat 2019 and Muga 2021 surveys, and thirty-one in both the Llobregat 2020 and Ter 2020 surveys. For all the measurements, samples were collected 10–20 cm deep from the water surface layer using a beaker. Once collected, the particle size distribution was measured with a laser particle size analyser (Lisst-100x, Sequoia Inc., US), an instrument that is frequently used in the field and in the laboratory and has been found to be suitable for sampling either organic (Serra et al., 2002) or inorganic particles (Serra et al., 2001). In the present study, the Lisst-100x was used as if measuring samples in the laboratory, hence a special 100 mL maximum capacity measuring cell was used. The Lisst-100x uses the laser diffraction theory of light to measure the volumetric particle size distribution of a suspension of particles. This technique requires a laser beam passing though the suspension of particles and scattering light in different angles. A series of 32 detector rings receive the scattered light. Each detector, situated at different angles, is associated to a certain particle size. The amount of light received by each detector is proportional to the concentration of said particle diameter. With its 32 log spaced size classes, the Lisst-100x determines the concentration of particles within the range of 2.5–500 μm. To calculate the particle concentration in a certain range of particle sizes, the sum of the concentration for the different particle diameters was considered.

Table 1
Details of the experimental conditions and measurements in each river survey: duration of the flood, total water volume discharged in the four cases studied, with or without sediment-replenishment, suspended sediments measured, and sediment traps deployed.

River survey	Llobregat 2019	Llobregat 2020	Ter 2020	Muga 2020
Duration (h)	9	10	24	10
Total water volume discharged (hm^3)	1.08	1.28	1.90	0.83
Sediment-replenishment	Yes	No	Yes	No
Suspended sediments measurements	Yes	Yes	Yes	Yes
Sediment traps deployed	No	Yes	Yes	Yes

2.4. Sediment-replenishment

Both surveys carried out in the Llobregat River were conducted at the same measuring point situated downstream from the La Baells reservoir (Fig. 1b). In the Llobregat 2019 survey, a total mass of 50 Tn of sediment was replenished upstream of the sampling position (Fig. 1b). A backhoe was used to artificially introduce the sediment into the river during the flood event. The sediment injection started when the flood reached its peak flow and lasted for one hour. The same procedure was used for the 25 Tn sediment-replenishment in the Ter 2020 flood. In both locations, sediment-replenishment was performed just below the dam to obtain greater mobilization of the sediment (Katano et al., 2021). Above the measuring point in the Ter River, two other tributaries - the Brugent and Osor rivers - feed into the river (Fig. 1b). As the sediment was collected from an area near the stream channel its characteristics were close to those that would occur in a natural peak flow inundating the riverbank areas near the channel. The sediment used for the replenishment in the Llobregat 2019 survey was made up of two particle size ranges: $d < 6$ μm and 6 μm $< d <$ 100 μm (Fig. 3a), with the greatest percentage corresponding to particles in the 6 μm $< d <$ 100 μm size range. In contrast, the sediment used for the replenishment study in the Ter 2020 survey had three particle size ranges: $d < 6$ μm, 6 μm $< d <$ 100 μm and $d >$ 100 μm (Fig. 3a) with the greatest percentage of particles corresponding to $d >$ 100 μm. In both surveys, the sediment was composed mainly of fine particles<500 μm in diameter (silts and fine and medium sands, Fig. 3b). The median of the grain size in the Ter River survey was 49.5 μm, whereas in the Llobregat River it was 37.9 μm (Fig. 3b).

2.5. Methods for measuring the particle sedimentation

Four sets of sediment traps were deployed at different water depths, which were determined by the study site in question (Table 2), except

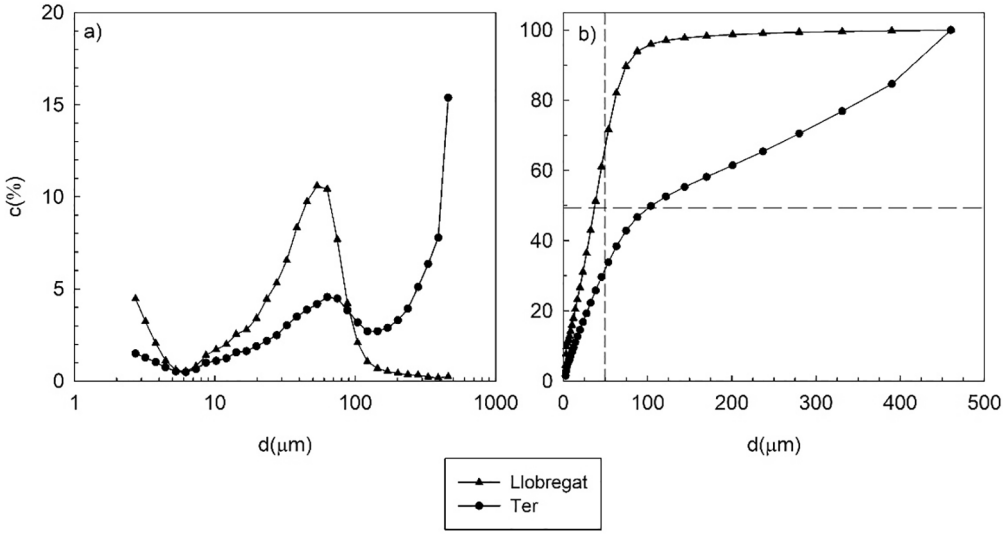

Fig. 3. a) Particle size distribution based on the volumetric particle concentration (c, in %) and b) cumulative particle distribution (c, in %) for the sediment used for the replenishment for the 2019 Llobregat River survey and for the 2020 Ter River survey.

Table 2
Depths (above the bottom, in m) of the sediment traps for each survey. For the 2019 Llobregat River survey no sediment traps were able to be deployed.

Llobregat 2020	Ter 2020	Muga 2021
0.70	0.18	0.05
0.90	0.38	0.25
1.10	0.58	0.45
1.30	0.78	0.65

for the Llobregat 2019 study where no sediment traps were able to be deployed. In addition, the deepest sediment trap in the Muga survey was lost and so no data was obtained for that particular depth. The sediment traps consisted of glass tubes 1.8 cm in diameter and 10 cm long, tied to a wire with three arms that allowed for three replicates per each depth. The aspect ratio of the tubes (height to diameter) was 5.6, like those used by Serra et al. (2021) and in accordance with the range of aspect ratios (length/diameter = 3–6) recommended by Håkanson et al. (1989). The sediment traps were deployed before and then collected after the flood event. Samples were transported to the laboratory and immediately stored in a refrigerator until they could be processed. The content of each tube was subsequently poured into a beaker and dried in an oven at 120 ℃ for 24 h. The dried sediment samples were then passed through a sieving kit with eight mesh sizes: 45 μm, 63 μm, 125 μm, 250 μm, 500 μm, 1 mm, 2 mm, and 4 mm. The mass collected by each sieve was then weighed, and the mass per square meter and day were determined for each location and depth and for each particle size range, which allowed for the particle size distribution deposited to be obtained (in gm^{-2} day^{-1}). The total dry mass deposited per unit area and time was obtained by summing the dry mass for all mesh sizes (in g m^{-2} day^{-1}).

2.6. Flood measurements

2.6.1. Hysteresis curves and hysteresis index

The hysteresis index (HI) can be calculated from the c-Q curves and is a numerical indicator of the hysteresis (Sherriff et al., 2016). To calculate it, the midpoint of Q (Q_{mid}) is firstly determined using:

$$Q_{mid} = 0.5(Q_{max} - Q_{min}) + Q_{min} \quad (1)$$

where Q_{max} and Q_{min} are the maximum and minimum flows, respectively. The corresponding values of c at the rising c_R and falling c_F branches of the loop at the Q_{mid} values can then be obtained (Sherriff et al., 2016). In this case, for $c_R > c_F$.

$$HI = (c_R/c_F) - 1 \quad (2)$$

and for $c_R < c_F$.

$$HI = (-1/(c_R/c_F)) + 1 \quad (3)$$

High HI indicates a high asynchronous pattern. HI > 0 indicates clockwise hysteresis, whereas HI < 0 indicates anticlockwise hysteresis. HI ~ 0 indicates a synchronous hysterical pattern. However, in the present study, and to compare watersheds, the normalized HI (HI_{norm}) will be considered (Le Cao et al., 2021). In such a case, the Q_{norm} and c_{norm} are calculated as:

$$Q_{norm} = \frac{Q - Q_{min}}{Q_{max} - Q_{min}} \quad (4)$$

$$c_{norm} = \frac{c - c_{min}}{c_{max} - c_{min}} \quad (5)$$

with such normalizations $Q_{norm\text{-}mid} = 0.5$ can be obtained introducing equations (4) and (5) into (1). Hi_{norm} can be calculated as:

$$HI_{norm} = c_{norm-R} - c_{norm-F} \quad (6)$$

where $c_{norm\text{-}R}$ and $c_{norm\text{-}F}$ are the normalized values of the concentration in the rising and falling limbs at $Q_{norm\text{-}med} = 0.5$, respectively. Since the flow in the surveys was not measured at the point of study, the water level was measured and used as a proxy for the temporal evolution of the flood. The water level was measured with a pressure sensor (Seabird 37, Seabird Instruments, US) installed at the measurement point (red point in Fig. 1 for each location). The sensor measured the water level to an accuracy of 0.1% of the full range and at a frequency of 0.7 Hz. The normalized water depth was considered:

$$z_{norm} = \frac{z - z_{min}}{z_{max} - z_{min}} \quad (7)$$

where z_{min} and z_{max} are the minimum and maximum water levels measured by the pressure sensor. Therefore, in the present study, $c_{norm\text{-}R}$ and $c_{norm\text{-}F}$ are the normalized values of the concentration in the rising and falling limbs, respectively, at $z_{norm\text{-}med} = 0.5$.

Floods are also further characterised by the flushing index (FI) that can be calculated as (Vaughan et al., 2017):

$$FI = c_{zmax,norm} - c_{zinitial,norm} \quad (8)$$

where $c_{zmax,norm}$ and $c_{zinitial,norm}$ are the normalized sediment concentrations at the peak of and at the beginning of the flood, respectively.

FI also ranges from −1 to 1. Negative FI values indicate a diluting effect of the rising limb of the hydrograph, whereas positive values indicate an increase in the sediment concentration on the rising limb.

3. Results

The particle size distribution of the suspended sediment (SS) concentration at the maximum flow was divided into three particle ranges: A (d < 6 μm), B (6 μm < d < 100 μm) and C (d > 100 μm) for all the surveys carried out (Fig. 4a-c). The greatest concentration corresponded to range B for all the surveys except the Llobregat 2019 survey (Fig. 4a), where the volumetric concentration of range C had very high values. The smallest concentration corresponded to the Muga River flood (Fig. 4d). The temporal evolution of the total volumetric concentration was found to present a fast increase at the head of the flood (Fig. 5 a, b and c) for all three particle ranges studied. For the Llobregat 2019 survey, the concentration of particles in range C presented the highest volumetric concentrations (Fig. 5a). For the Llobregat 2020 and Ter 2021 surveys, the greatest volumetric concentration corresponded to range B, which peaked at the time of the maximum flow. Except for the Ter 2020 flood, after the arrival of the head of the flood, the temporal evolution of the volumetric concentration presented a plateau that remained nearly constant before starting to decrease again (Fig. 5b and c). The volumetric concentration for the Muga flood was far smaller than that for the other floods, including the one in the Llobregat 2020 without sediment-replenishment. The concentration of particles in range B was slightly above that of range C. The concentration of these two particle ranges in this survey remained below 20 μL L^{-1}, whereas in the other floods it reached values above 20 μL L^{-1}.

The hysteresis curves of each flood and for each particle range present a clockwise or anticlockwise circulation depending on the case. For the 2019 Llobregat River survey, the circulation of the hysteresis curve was clockwise for all the particle size ranges (Fig. 6a-c). The same behaviour was observed for the Llobregat 2020 survey for the three particle size ranges (Fig. 6d-f). For the 2020 Ter River survey, the hysteresis curve was an eight-figure loop for the three particle ranges (Fig. 7a-c). For the Muga River flood, the hysteresis curve presented again a clockwise circulation for the three particle size ranges (Fig. 7d-f).

The hysteresis index, calculated for each flood and particle range, is presented in Table 3. The hysteresis index for the two surveys in the Llobregat and Muga rivers had positive values, except for the largest particle range (range C) in the 2019 Llobregat River flood. In this case, the hysteresis index was negative, albeit with a very low value. In the case of the Ter River flood, the hysteresis index was negative for all the particle ranges (Table 3). Note that the hysteresis index for the surveys with replenishment (Llobregat 2019 and Ter 2020) presented smaller values for all the particle ranges compared to those for the without sediment-replenishment experiments (Llobregat 2020 and Muga 2021). The flushing index showed a great variability between watersheds and particle sizes (Table 3) with the highest FI being obtained for the Ter River survey that was carried out with replenishment. High FI values were likewise obtained for the medium particle size range 6 μm < d < 100 μm compared to the other particle sizes. In nearly all the surveys, and for all particle sizes, the flood was clockwise flushing dominated; except for the case of the Ter where it was an anticlockwise flushing type ($HI_{norm} < 0$, Fig. 8). For the largest particle range of d > 100 μm from the 2019 Llobregat River survey, the flood was anticlockwise diluting, i.e., with negative FI and HI_{norm} indices. The relationship between HI_{norm} and FI had a high variability between surveys and particle sizes. However, those surveys corresponding to the cases with sediment-replenishment had nearly constant FI.

Once the head of the flood had passed by and the discharge had started to decrease, the total SS volumetric concentration also decreased gradually in all cases and for all particle ranges. After the head, all the discharges presented a linear trend between c and z (Fig. 9a-f). This linear trend was considered to fit the data and the slopes were thus calculated (see Table 4). The Ter 2020 survey with sediment-replenishment had the greatest slope, indicating a greater SS concentration for the same flows (Table 4). In contrast, the lowest slopes were found for the Muga 2021 survey that did not have sediment-

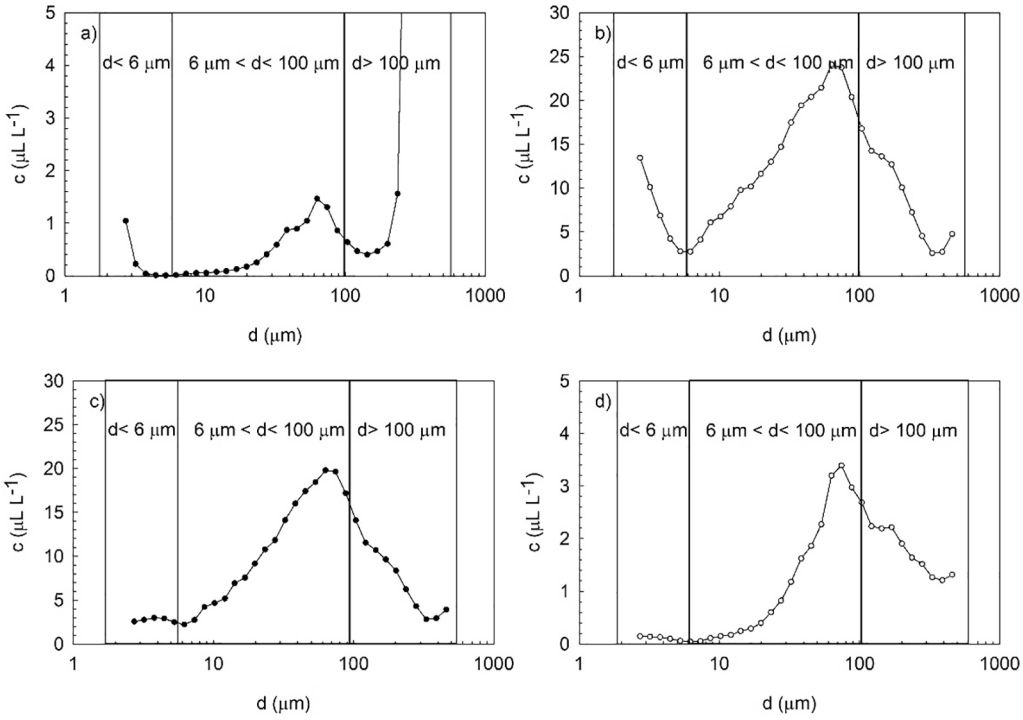

Fig. 4. Volumetric sediment particle size distribution for each survey carried out: Llobregat 2019 a), Llobregat 2020b), Ter 2020c) and Muga 2021 d). These particle distributions correspond to the time when the maximum flood was observed (see Fig. 3) for each survey. Solid symbols correspond to discharges with sediment-replenishment and empty symbols to discharges without sediment-replenishment.

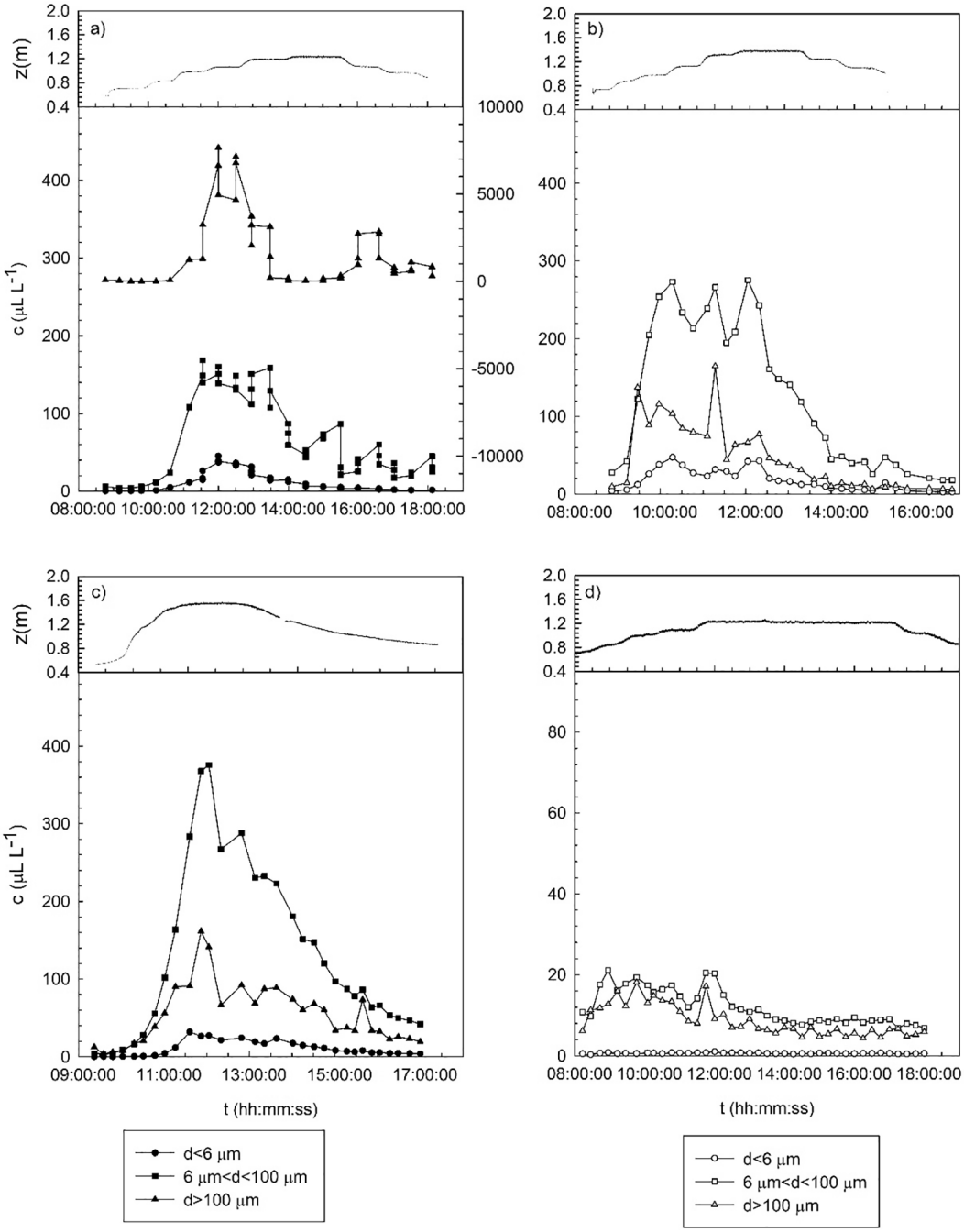

Fig. 5. Temporal evolution of the sediment concentration for the three particle sizes considered in the study for each survey carried out: Llobregat 2019 a), Llobregat 2020b), Ter 2020c) and Muga 2021 d). The temporal evolution of the water level at the measuring point has also been plotted at the top of each figure. Solid symbols correspond to floods with sediment-replenishment and empty symbols to floods without sediment-replenishment.

replenishment. The slope found for the Llobregat 2019 survey with sediment-replenishment and for particle range A, was slightly above that found for the Llobregat 2020 survey without sediment-replenishment. However, for the particles in range B, the Llobregat 2019 survey with sediment-replenishment had a greater slope than that of the Llobregat 2020 without sediment-replenishment. For the Muga River survey, the smallest particle range, presented a small slope that was not significant ($p > 0.05$).

The dry mass deposited at each depth and for each site is plotted in Fig. 10. The particle size distribution of the sediment deposited was bimodal for the Llobregat 2020 survey (Fig. 10a), with a maximum in the range of 63 μm – 250 μm and another in the range of 500 μm – 4000 μm. DS (deposited sediment) increased with depth for all the size classes studied. The maximum concentration for the peak in the range 63 μm – 250 μm was lower than that for the peak in the range 500 μm – 4000 μm. In contrast, DS for the Ter 2020 survey presented mainly one peak centred in the range 250 μm – 2000 μm (Fig. 10b), with the greatest mass per unit area and time when compared to the other two surveys. DS for the Muga River 2021 survey also presented a bimodal distribution with two maximums: one in the range 63 μm – 1000 μm and another in the range 1000 μm – 4000 μm (Fig. 10c). The DS of the second peak was far below that of the first peak. Again, in both the Ter 2020 and Muga 2021 surveys, DS increased with depth for all the particle size ranges studied. The DS for the Muga was the smallest compared with the other two surveys. The DS increased with depth for all the surveys carried out (Fig. 10d).

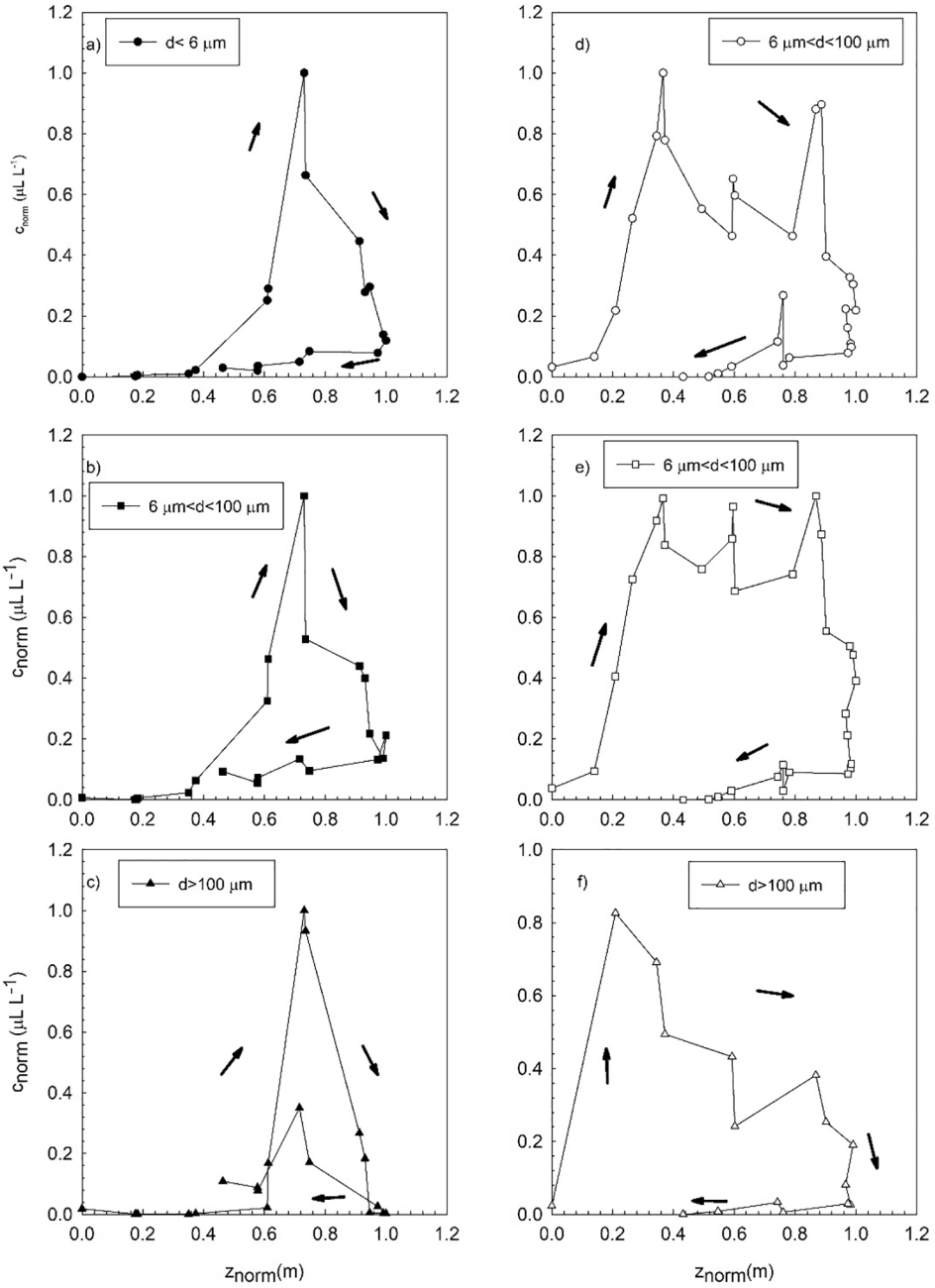

Fig. 6. Hysteresis plot of the volumetric sediment concentration for each particle diameter range versus the water level (z in m). Left panels correspond to the Llobregat 2019 survey and right panels to the Llobregat 2020 survey. Solid symbols correspond to floods with sediment-replenishment and empty symbols to floods without sediment-replenishment.

4. Discussion

The artificial flood from the three reservoirs transported suspended sediment downstream. The flooding events, which are dictated by legislation (Agència Catalana de l'Aigua (ACA), 2005), were characterised by different peak flows and hydrographs according to the characteristics and hydrological regimes of each river.

4.1. Hysteresis curves of the different suspended sediment particles transported by the flood with and without sediment-replenishment

The particles transported in each flood differed between watersheds. In the Llobregat, the greatest percentage of SS particles transported were with diameters d > 100 μm (with 88.22%) in the sediment-replenishment case in the 2019 survey. However, it should be noted that a high volume concentration of large particles usually represents a low number because, as opposed to small particles, large particles make a higher contribution to the particle volume representation. In contrast, for the without-replenishment case the particles in the 6 μm < d < 100 μm size range had the highest percentage (68.76%). For the Ter River survey (with replenishment), the greatest percentage of SS particles transported likewise corresponded to particles in the 6 μm < d < 100 μm size range (72.35%), as was also found in the Muga (without replenishment) 57.76%. In the with-replenishment Llobregat survey, the percentage of larger particles corresponded to the transport of a few large particles with the flow that accounted for a high contribution to the volumetric particle concentration. The volumetric particle distributions were three-modal in all floods. The temporal evolution of the volumetric

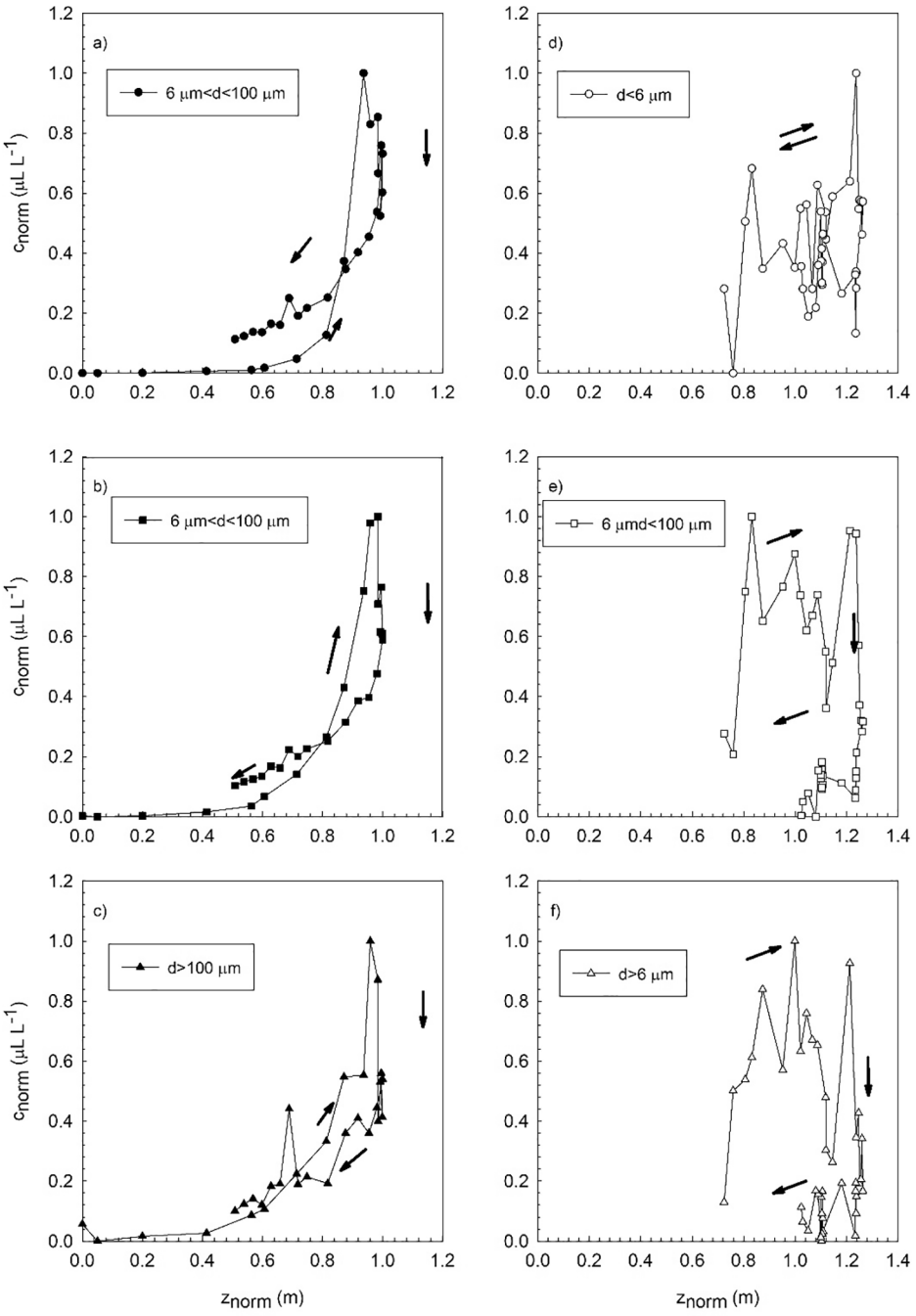

Fig. 7. Hysteresis plot of the volumetric sediment concentration for each particle diameter range versus the water level (z in m) at the point of measurement. Panels on the left correspond to the Ter 2020 survey and on the right to the Muga 2021 survey. Solid symbols correspond to floods with sediment-replenishment while empty symbols correspond to floods without sediment-replenishment.

Table 3
Hysteresis index and flushing index values calculated from equation (6) for the different surveys carried out and for the three different particle ranges considered (d < 6 μm, 6 μm < d < 100 μm, d > 100 μm).

	Survey	d < 6 μm	6 μm < d < 100 μm	d > 100 μm
HI	Llobregat 2019	0.11	0.12	−0.09
	Llobregat 2020	0.55	0.76	0.46
	Ter 2020	−0.10	−0.07	−0.01
	Muga 2021	0.07	0.56	0.83
FI	Llobregat 2019	0.12	0.20	−0.02
	Llobregat 2020	0.19	0.35	0.14
	Ter 2020	0.73	0.59	0.48
	Muga 2021	0.29	0.04	0.04

SS particle concentration of the three particle ranges peaked at the peak flow. In some cases, the particle volume evolution presented a plateau at the maximum flow that was maintained with time during the time the flood remained high and started to decrease gradually in the falling limb of the hydrograph. However, for the Ter River, the maximum SS particle volume concentration was achieved at the arrival of the head of the flood, although shortly after this point the SS particle volume concentration gradually decreased. This result might be associated to the supply of sediment sources being situated far from the measuring position, i.e., two Ter River tributaries situated upstream of the measuring station. Those two sources were only able to begin to supply sediment when the flow was high.

Hysteresis curves c-z indicate the temporal evolution of the SS

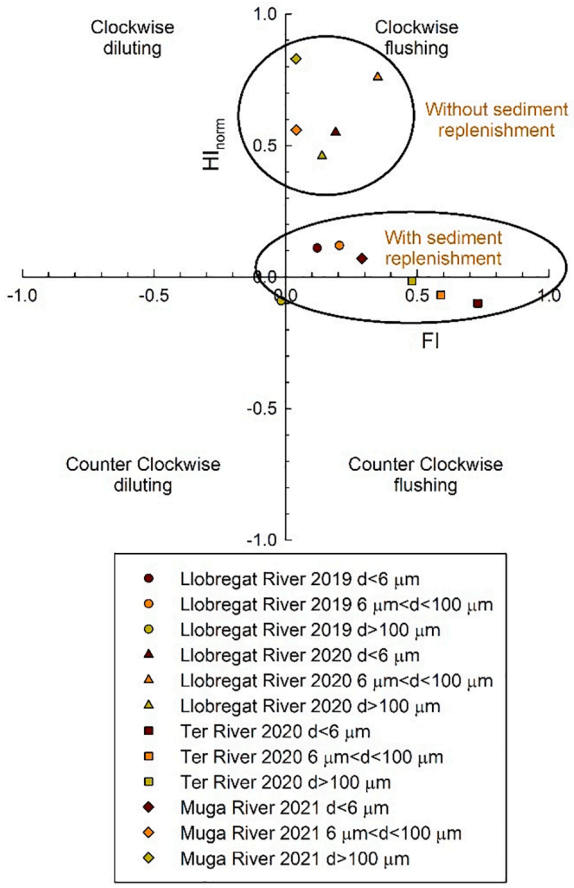

Fig. 8. Normalized hysteresis index (HI_{norm}) versus the flushing index (FI) for the different floods studied and for the different particle sizes considered.

transport relative to the temporal evolution of the flood (in the current study we used the water level at the measuring point as a proxy, see Methods). In addition, curves c-z provide information on the provable sources of the particles. These curves might present different patterns that are associated to different behaviours in the transport of sediment in the watershed (see Methods). C-z curves have been plotted for each particle size range ($d < 6$ μm, 6 μm $< d < 100$ μm and $d > 100$ μm) to understand the different transport mechanisms of each particle size range. For the Llobregat, the three types of particles presented a clockwise circulation of the c-z plot, indicating that the riverbed becomes cleaner with the flood on the event's recession, i.e., that the flood transports all the particles deposited on the catchment downstream, thus remaining depleted of them (Haddadchi and Hicks, 2021). In other words, eroding the fine particles deposited on the bed. Hamshaw et al., (2018) studied long-term data from six sites in the Mad River (Green Mountains, Vermont, USA) and found that 90% of the floods presented hysteretic loops with clockwise circulation being the most common type. From the current study, the Llobregat 2020 flood presented a pronounced clockwise loop, whereas the hysteretic loop for the Llobregat 2019 flood was less pronounced. This difference was attributed to the latter being carried out with sediment-replenishment. Clockwise hysteresis loops have been observed for sediment-associated metals during floods in a small catchment (Rodríguez-Blanco et al., 2018). In their work, hysteresis loops indicate that the source of sediment-associated metals was close to the river network and was easily mobilised in the rising limb and depleted in the falling limb of the hydrograph by each event.

In this study, positive HI has been found for these loops in the Llobregat River, except for the case of $d > 100$ μm in the 2019 survey (with replenishment). However, greater HI values were found for the case without replenishment. This could be the result of a greater sediment depletion in the without-replenishment case compared to the with-replenishment case that presented lower HI. Sediment-replenishment did not modify the c-z loops of the flood in the Llobregat River surveys. However, for the surveys where sediment-replenishment was carried out, the HI of the flood was low, resulting in a more balanced sediment transport behaviour, i.e., reducing the difference of c between the rising and falling limbs of the hydrograph (Haddadchi and Hicks, 2021). Positive HI was found for the evolution of total suspended solids in floods in White Clay Creek (Delaware, USA), indicating a strong clockwise hysteresis pattern and signalling mobilization of within-the-channel source areas (Rose et al., 2017).

For the Ter River, (i.e., with replenishment) the c-z loop had an eight-shape figure (a clockwise loop combined with an anticlockwise loop). This indicates that, at high water flows, more sediment sources are supplying sediment to the flood. The HI index is negative for all the particle ranges, indicating a similar behaviour between them. However, the smallest particle range presented the greatest negative HI, probably indicating that the supply of these particles was from sources situated farther away and was greater than that for the medium and large particle size ranges. For the largest particles, the HI index was still negative, albeit presenting a very low value, indicating that the transport of these particles was nearly balanced (Haddadchi and Hicks, 2021). In other words, the transport in the rising limb of the hydrograph was close to that for the falling limb of the hydrograph. Note that the balanced transport of sediment could be attributed to the fact that this survey was carried out with sediment-replenishment.

For the Muga River, the behaviour of the finest particles differed from that of the other two particle size ranges. For $d < 6$ μm, HI was nearly zero, indicating a balanced transport of this particle-size range. In this case, the supply of these type of particles from other sources that mobilized the sediment at high water flows might be the reason for a balanced transport without sediment depletion of fine particles in the river catchment. In contrast, sediment particles in the ranges 6 μm $< d <$ 100 μm and $d > 100$ μm presented a high positive HI index, indicating a depletion of sediment, i.e., transport of these particles from the riverbed downstream. The cases of low HI, like that of the Ter survey with replenishment for $d > 100$ μm and that of the Muga River for $d < 6$ μm, have been associated with an uninterrupted sediment supply throughout the flood (Williams, 1989). In the current study, the smallest river catchment (Muga River) studied presented clockwise hysteresis loops, coinciding with the results of previous studies that claim that such hysteresis loops are characteristic of small rivers (Seeger et al., 2004; Smith and Dragovich, 2009). However, Haddadchi and Hicks (2021) show that anticlockwise and eight-figure loops could also occur in small catchments. They indicate that there are other morphological aspects of the rivers, such as river slopes, soil erodibility and sediment sources, that must be considered. In addition, the connectivity along a river network also explains the movement or the storage of sediment into river channels. Wider river channels or low gradient slope segments can produce sediment accumulation in river areas (Wohl et al., 2015).

The two without sediment-replenishment surveys carried out in this study corresponded to the clockwise flushing type, with positive HI_{norm} and positive FI indicating that the SS transported corresponded to the riverbed sites near the point of study. However, studies carried out with sediment-replenishment had low HI_{norm}, indicating a balanced sediment transport independent on the flushing index FI. The 2020 Ter River survey had high FI values, indicating a high sediment transport in the rising limb of the flood for all particle sizes, but negative HI_{norm}, indicating that the sources of sediment were from sites situated far from the point of study.

4.2. Transport of sediment particles by the river flood with and without sediment-replenishment

The concentration of transported particles in the falling limb of the

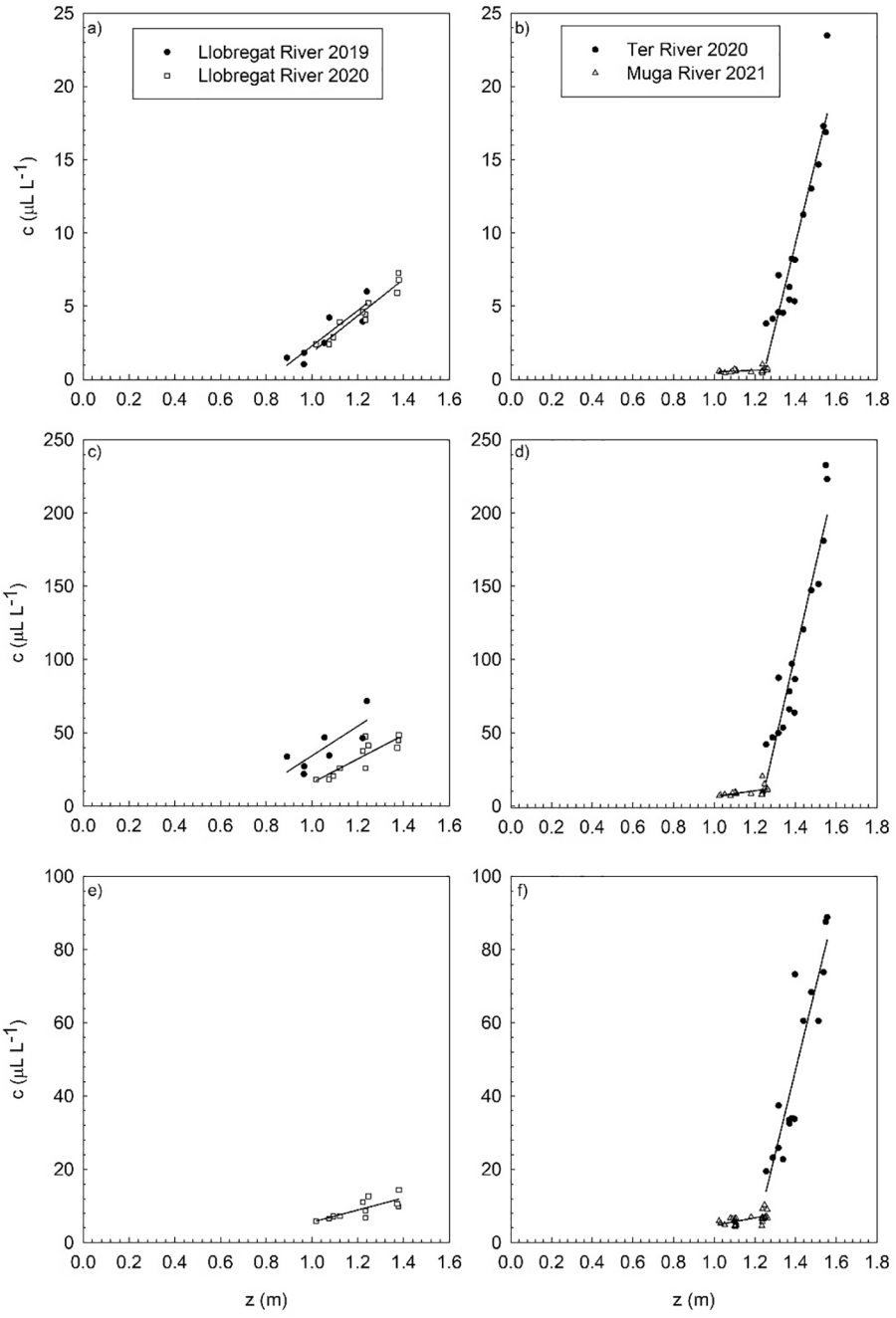

Fig. 9. Volumetric SS concentration for each particle diameter range versus the water level (z in m) in the falling limb of the hydrograph for the different particle size ranges considered and for the different surveys carried out. Solid symbols correspond to floods with sediment-replenishment while empty symbols correspond to floods without sediment-replenishment.

flood presented a linear relationship with the water level. The slopes of a linear fitting indicate the effect the flood has on the transport of sediment of each particle size (Williams, 1989). The survey with the greatest slope for all the particle size ranges was the Ter River 2020 case. In the case of the Llobregat surveys, the smallest particles with d $<$ 6 µm presented similar slopes with similar ranges of minimum and maximum values. Therefore, the sediment- replenishment for this type of particle did not present high differences in the falling limb of the flood. In contrast, for the medium-size particle range, the slope was 23.9% greater for the Llobregat 2019 survey than for the Llobregat 2020. This indicates that the transport of sediment in the falling limb was greater for the case of sediment-replenishment. When comparing the two cases of sediment-replenishment, and for the case of the smallest particle size range, the transport of particles was 370% greater for the Ter River than for the Llobregat. For the medium-size particle range, the transport of sediment particles was 645.3% greater in the Ter than in the Llobregat 2019. This indicates that these particles are better mobilized in the Ter catchment area than in the Llobregat catchment. This result might be attributed to the fact that in the Ter River the peak flow was greater than that in the Llobregat 2019 (Table 1). The Muga River presented slopes of c-z in the falling limb far smaller than those in the other catchments for all the particle size ranges analysed, indicating a lower transport of sediment particles in the falling limb of the flood. In addition, when comparing the maximum concentration between the surveys, the Muga River transported fewer suspended sediments than the other rivers, including the Llobregat 2020 survey without sediment injection. This

Table 4
Values of the parameters (m, m_{min}, m_{max}, R^2 and *p*-value) of the fitting curves of Fig. 9, where m is the slope, m_{min} and m_{max} are the minimum and maximum values of the slope based on the 95% confidence, and R^2 is the correlation coefficient.

		Llobregat 2019	Llobregat 2020	Ter 2020	Muga 2021
d < 6 μm	m	12.06 ($p < 0.05$)	17.99 ($p < 0.05$)	56.76 ($p < 0.05$)	0.56 ($p > 0.05$)
	m_{min}	5.10	8.63	43.99	−0.04
	m_{max}	19.0	27.36	68.53	1.164
	R^2	0.758	0.584	0.857	0.101
6 μm < d < 100 μm	m	100.80 ($p < 0.05$)	127.33 ($p < 0.05$)	606.26 ($p < 0.05$)	19.06 ($p < 0.05$)
	m_{min}	15.30	56.88	478.50	6.54
	m_{max}	186.30	197.78	734.06	31.59
	R^2	0.577	0.553	0.872	0.271
d > 100 μm	m	–	27.89 ($p > 0.05$)	228.45 ($p < 0.05$)	10.39 ($p < 0.05$)
	m_{min}	–	10.32	167.47	3.96
	m_{max}		45.45	289.43	16.81
	R^2	–	0.483	0.809	0.298

might be due to the lower peak flow in the Muga River compared to the other rivers.

The maximum sediment concentration in each flood was 561.33 μL L^{-1} in the 2020 Ter River survey, 387.12 μL L^{-1} in the 2020 Llobregat River survey, 8021.95 μL L^{-1} in the 2019 Llobregat River survey and 38.44 μL L^{-1} in the 2021 Muga River survey. Considering a typical density of 2.5 kg L^{-1} for the sediment, this represents a mass concentration of 1.4 g L^{-1}, 0.97 g L^{-1}, 20 g L^{-1} and 0.10 g L^{-1}, respectively. These values are in the range of the mass concentrations observed in flooding events in Mediterranean intermittent rivers that ranged between 0 and 35.6 g L^{-1} (Fortesa et al., 2021). The events with the highest sediment transport corresponded to the most energetic events, i.e., those with the highest water flows, which is also in accordance with the results of Fortesa et al. (2021). Moreover, sediment-replenishment events (Llobregat 2019 and Ter 2020 surveys) also increased the amount of SS transport.

4.3. Particle sedimentation during the floods with and without sediment-replenishment

Sedimentation of particles in the without sediment-replenishment Llobregat survey was found to present a bimodal distribution, with one range of particles being 45 μm < d < 500 μm corresponding to fine and medium sands, and a second range of 500 μm < d < 4000 μm

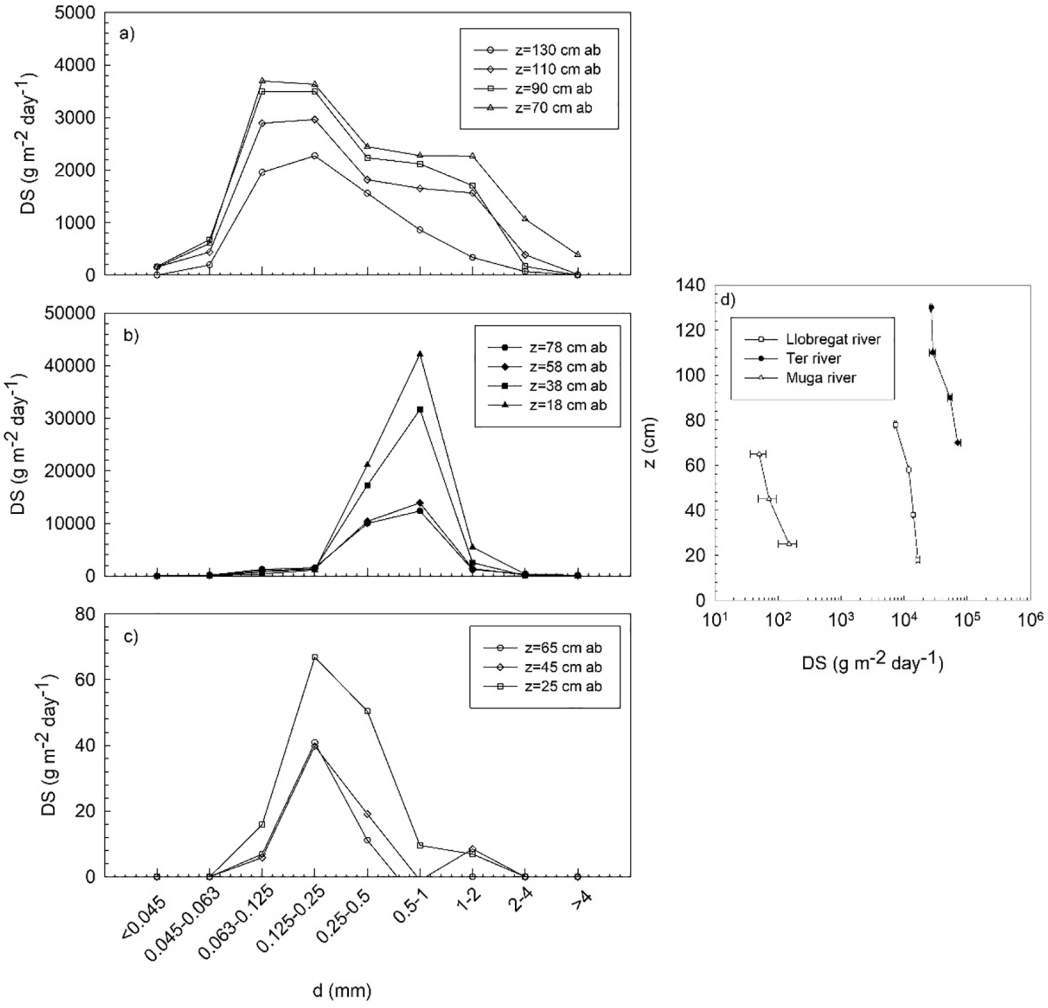

Fig. 10. Particle distribution of the deposited sediment (DS in g m^{-2} day^{-1}) for a) the 2020 Llobregat River survey, b) the 2020 Ter River survey and c) the 2021 Muga River survey. d) Total mass of deposited sediment (DS_T, in g m^{-2} day^{-1}) for the different depths where the sediment traps were situated for the three surveys. Solid symbols correspond to floods with sediment-replenishment, empty symbols correspond to floods without sediment-replenishment, and ab in the legends stands for 'above the bottom'.

corresponding to coarse sand and fine gravel (Blott and Pye, 2012). The first range presented a greater concentration per unit time and area greater than the second particle size range. The particles that settled and were collected by the trap situated in the shallowest depth were only from the smallest range. This coincides with the fact that the transported particles measured with the laser particle size analyser had their greatest concentration in this size range. In contrast, in the Ter River, and with sediment-replenishment, the mass of settled particles was higher than that of the Llobregat without replenishment. The sedimentation of larger particles and with greater concentrations in this survey might be the result of the replenishment in the Ter survey. This particle size range was outside the measuring range of the laser particle size analyser and so its transport via the flood could not be determined. In the Muga River survey, the distribution of the settled sediment was also bimodal with a large sedimentation of the smallest range and a very small sedimentation of particles of larger diameters. The concentrations were far smaller than those for the other two floods. This result might be explained by the fact that the case of the Muga survey had a peak flow between 0.36 and 0.54 times the other two watersheds. Furthermore, there was no sediment-replenishment. The vertical profile of particle sedimentation presented an increase of the mass per unit area and time increasing with depth, according to a typical sedimentation profile. Again, the with-replenishment Ter survey presented the highest particle sedimentation followed by the other two without-replenishment cases: Llobregat 2020 and Muga 2021. The total deposited sediment was one order of magnitude higher in the Ter River compared to the 2020 Llobregat River, which might be because of the replenishment plus the contribution of the high water flow. The without-replenishment Llobregat survey presented a total sediment deposition two orders of magnitude higher than that of the Muga River, also without replenishment. This difference can be attributed to the higher peak flow of the discharge in the Llobregat 2020 survey.

4.4. River management strategies for enhancing sediment transport downstream of a dam

Water release and sediment-replenishment have been found to be the main drivers for the transport of SS in the studied rivers and also on the impact of sedimentation. High water flows produced a high sediment transport in all the catchments. Sediment-replenishment produced a more balanced sediment transport and higher sedimentation rates than without sediment-replenishment, indicating that the river catchment is not depleted of sediment when a flood with sediment-replenishment is performed. Therefore, from the results found in this study, sediment-replenishment should be performed under the higher flow artificial floods. In such situations, sediment-replenishment would prevent the depletion of sediment in riverbeds.

Therefore, this study shows that hysteresis curves c-z and sedimentation records can provide information on the impact of artificial floods and sediment-replenishment management have on soil and water conservation strategies in different catchments. It must be pointed that the response of rivers to flow variability cannot be attributed to a single isolated episode (Konrad et al., 2011). Instead, long-term river responses are associated to sequences of flows over long time-periods. Consequently, future work still needs to be done to determine the long-term impact sediment-replenishment and water release might have on the different watersheds. Moreover, the current study presents data on suspended sediment transport and sedimentation at one measuring point along the river. Further work should be done to determine the longitudinal transport of suspended sediment and sedimentation at downstream river stations to obtain more detailed information on the impact that both flood and sediment-replenishment strategies have on river and coastal ecosystems.

5. Conclusions

Hysteretic loops have been used in the current study to determine and compare the transport of suspended sediment of different particle sizes in river floods. For the same water flow, particles with different sizes are transported differently. Although clockwise hysteretic loops were observed in the cases of the Muga and Llobregat Rivers, in the Ter River anticlockwise circulations prevailed for all the particle sizes.

Sediment-replenishment floods (performed in the Llobregat and Ter rivers) have also been compared to non-sediment-replenishment floods (performed in the Llobregat and the Muga rivers). Hysteresis loops have not changed their circulation patterns whether the floods were performed with or without sediment-replenishment. However, all the cases with sediment-replenishment had normalized hysteresis indices close to zero, much lower than those carried out without sediment-replenishment, indicating that sediment-replenishment produced a more balanced suspended sediment transport during the flood process. In contrast, in floods without sediment-replenishment, a depletion of suspended sediment was observed in the falling limb of the flood. This indicates that the flood washed out the fine particles deposited in the river catchment. In addition, sedimentation rates were greater in sediment-replenishment than without sediment-replenishment cases. Therefore, sediment-replenishment provides a management strategy or tool to prevent riverbeds being washed out after artificially induced floods downstream of a dam.

The current study is focused on the results obtained from one point along the different rivers' trajectories. To obtain detailed information on the sedimentation rates along a river's course, new studies with and without sediment-replenishment need to be performed with measurements at different points along rivers situated downstream of a dam. Moreover, more work should be done in the future to determine the long-term effects sediment-replenishment strategies have on artificial floods in river hydrology, sediment transport and also on its ecological status. It might also be interesting to include other important parameters in the study such as soil erodibility and the river slope with and without sediment-replenishment strategies. This will add more information to finally determine in what situations sediment-replenishment could be used as a best river restoration practice.

CRediT authorship contribution statement

Teresa Serra: Conceptualization, Methodology, Formal analysis, Investigation, Writing – original draft, Writing – review & editing, Data curation. **Marianna Soler:** Investigation, Methodology. **Aina Barcelona:** Investigation, Methodology. **Jordi Colomer:** Investigation, Conceptualization, Methodology, Writing – review & editing.

Declaration of Competing Interest

The authors declare that they have no known competing financial interests or personal relationships that could have appeared to influence the work reported in this paper.

Acknowledgements

This research was funded by LABAQUA S.A. (Madrid, Spain). We are also grateful for the support given by the Agència Catalana de l'Aigua (ACA Barcelona, Spain) and Serbaikal Ingenieros S.L.L. (Madrid, Spain). This research was funded by the Ministerio de Economía, Industria y Competitividad of the Spanish Government through the grant CGL2017-86515-P. We are grateful to Prof. Josep Mas-Pla of the Department of Environmental Sciences of the University of Girona for providing detailed information of the morphology of the three rivers in the current study (Ter, Llobregat and Muga). Open Access funding was provided thanks to the CRUE-CSIC agreement with Elsevier.

References

Agència Catalana de l'Aigua (ACA), 2005. Sectorial maintenance flow plan for the Catalan watersheds (in Catalan: Pla sectorial de cabals de manteniment de les conques internes de Catalunya). Generalitat de Catalunya, Departament de Medi Amient i Habitatge.

Baisre, J.A., Arboleya, Z., 2006. Going against the flow: effects on river damming in Cuban fisheries. Fish Res. 81, 283–292.

Battisacco, E., Franca, M.J., Schleiss, A.J., 2016. Sediment replenishment: influence of the geometrical configuration on the morphological evolution of channel-bed. Wat. Resour. Res. 52 (11), 8879–8894.

Bösch, L., Battisacco, E., Franca, M.J., Schleiss, A.J., 2016. Influence of consecutive sediment replenishment on channel bed morphology. River Flow, Taylor and Francis Group.

Blott, S.J., Pye, KENNETH, 2012. Particle size scales and classification of sediment types based on particle size distributions: review and recommended procedures. Sedimentology 59 (7), 2071–2096.

Burroughs, B.A., Hayes, D.B., Klomp, K.D., Hansen, J.F., Mistak, J., 2009. Effects of Stronach dam removal on fluvial geomorphology in the Pine River, Michigan, United States. Geomorphology 110 (3-4), 96–107.

Cao, L., Liu, S., Wang, S., Cheng, Q., Fryar, A.E., Zhang, Z., Yue, F., Peng, T., 2021. Factors controlling discharge-suspended sediment hysteresis in karst basins, southwest China: Implications for sediment management. J. Hydrol. 594, 125792.

de Castro, L.S., de Souza Lopes, A.A., Coars, L., Palheta, L., de Souza Menezes, M., Fernandes, L.M., Dunck, B., 2021. Dam promotes downriver functional homogenization of phytoplankton in a transitional river-reservoir system in Amazon. Limnology. 22 (2), 245–247.

EC, 2000. EU Water Framework Directive.

García de Jalón, D., Bussettini, M., Rinaldi, M., Grant, G., Friberg, N., Cowx, I.G., Magdaleno, F., Buijse, T., 2017. Linking environmental flows to sediment dynamics. Water Policy 19, 358–375.

Fortesa, J., Ricci, G.F., García-Comendador, J., Gentile, F., Estrany, J., Sauquet, E., Datry, T., De Girolamo, A.M., 2021. Analysing hydrological and sediment transport regime in two Mediterranean intermittent rivers. Catena. 196, 104865.

Gabbud, C., Robinson, C.T., Lane, S.N., 2019. Summer is in winter: Disturbance-driven shifts in macroinvertebrate communities following hydroelectric power exploitation. Sci. Total Environ. 650, 2164–2180.

Gabbud, C., Lane, S.N., 2016. Ecosystem impacts of alpine water intakes for hydropower: the challenge of sediment management. WIREs Water 3 (1), 41–61.

Haddadchi, A., Hicks, M., 2021. Interpreting event-based suspended sediment concentration and flow hysteresis patterns. J. Soils Sed. 21 (1), 592–612.

Håkanson, L., Floderus, S., Wallin, M., 1989. Sediment trap assemblages – a methodological description. Hydrobiologia 176 (177), 481–490.

Hamshaw, S.D., Dewoolkar, M.M., Schroth, A.W., Wemple, B.C., Rizzo, D.M., 2018. A new machine-learning approach for classifying hysteresis in suspended-sediment discharge relationships using high-frequency monitoring data. Wat. Resour. Res. 54 (6), 4040–4058.

Itsukushima, R., Ohtuski, K., Sato, T., Kano, Y., Takata, H., Yoshikawa, H., 2019. Effects of sediment released from a check dam on sediment deposits and fish and macroinvertebrate communities in a small stream. Water. 11, 716.

Kantoush, S.A., Sumi, T., Kubota, A., Suzuki, T., 2010. Impacts of sediment replenishment below dams on flow and bed morphology of river. In: First International Conference on 'Coastal Zone Management of River Deltas and Low Land Coastlines', pp. 285–303.

Katano, I., Negishi, J.N., Minagawa, T., Doi, H., Kawaguchi, Y., Kayaba, Y., 2021. Effects of sediment replenishment on riverbed environments and macroinvertebrate assemblages downstream of a dam. Sci. Rep. 11, 7525.

Kondolf, G.M., Wilcock, P.R., 1996. The flushing flow problem: defining and evaluating objectives. Wat. Resources Res. 32 (8), 2589–2599.

Konrad, C.P., Olden, J.D., Lytle, D.A., Melis, T.S., Schmidt, J.C., Bray, E.N., Freeman, M. C., Giddo, K.B., Hemphill, N.P., Kennard, M.J., McMullen, L.E., Mims, M.C., Pyron, M., Robinson, C.T., Williams, J.G., 2011. Large-scale flow experiments for managing river systems. Bioscience 61, 948–959.

Lehner, B., Liermann, C.R., Revenga, C., Vörösmarty, C., Fekete, B., Crouzet, P., Döll, P., Endejan, M., Frenken, K., Magome, J., Nilsson, C., Robertson, J.C., Rödel, R., Sindorf, N., Wisser, D., 2011. High-resolution mapping of the world's reservoirs and dams for sustainable river-flow management. Front. Ecol. Environ. 9 (9), 494–502.

Magdaleno, F., 2017. Experimental floods: A new era for Spanish and Mediterranean rivers? Environ. Sci. Policy 75, 10–18.

Megnounif, A., Terfous, A., Ouillon, S., 2013. A graphical method to study suspended sediment dynamics during flood events in the Wadi Sebdou, NW Algeria (1973–2004). J. Hydrol. 497, 24–36.

Mulligan, M., van Soesbergen, A., Sáenz, L., 2020. GOODD, a global dataset of more than 38,000 georeferenced dams. Sci. Data. 7, 31.

Ock, G., Sumi, T., Takemon, Y., 2013. Sediment replenishment to downstream reaches below dams: implementation perspectives. Hydrological Research Letters. 7 (3), 54–59.

Poff, N.L., Allan, J.D., Bain, M.B., Karr, J.R., Prestegaard, K.L., Richter, B.D., Sparks, R.E., Stromberg, J.C., 1997. The natural flow regime. A paradigm for river conservation and restoration. Bioscience 47 (11), 769–784.

Pokrovsky, O.S., Schott, J., 2002. Iron colloids/organic matter associated transport of major and trace elements in small boreal rivers and their estuaries (NW Russia). Chem. Geol. 190 (1–4), 141–179.

Rodríguez-Blanco, M.L., Soto-Varela, F., Taboada-Castro, M.M., Taboada-Castro, M.T., 2018. Using hysteresis analysis to infer control son sediment-associated and dissolved metals transport in a small humid temperate catchment. J. Hydrol. 565, 49–60.

Rose, L.A., Karwan, D.L., Godsey, S.E., 2017. Concentration-discharge relationships describe solute and sediment mobilization, reaction, and transport at event and longer timescales. Hydrol. Process. 32, 2829–2844.

Seeger, M., Errea, M.-P., Beguería, S., Arnáez, J., Martí, C., García-Ruiz, J.M., 2004. Catchment soil moisture and rainfall characteristics as determinant factors for discharge/suspended sediment hysteretic loops in a small headwater catchment in the Spanish Pyrenees. J. Hydrol. 288 (3-4), 299–311.

Sherriff, S.C., Rowan, J.S., Fenton, O., Jordan, P., Melland, A.R., Mellander, P.-E., Ó hUallacháin, D., 2016. Storm event suspended sediment-discharge hysteresis and controls in agricultural watersheds: implications for watershed scale sediment management. Environ. Sci. Technol. 50 (4), 1769–1778.

Smith, H.G., Dragovich, D., 2009. Interpreting sediment delivery processes using suspended sediment-discharge hysteresis patterns from nested upland catchments, south-eastern Australia. Hydrol. Process. 23 (17), 2415–2426.

Serra, T., Colomer, J., Cristina, X., Vila, X., Arellano, J.B., Casamitjana, X., 2001. Evaluation of a laser in situ scattering instrument for measuring the concentration of phytoplankton, purple sulphur bacteria and suspended inorganic sediments in lakes. J. Env. Eng. 127 (11), 1023–1030.

Serra, T., Colomer, J., Baserba, C., Soler, M., Casamitjana, X., 2002. Quantified distribution of diatoms during the stratified period of Boadella reservoir. Hydrobiologia 489, 235–244.

Stähly, S., Franca, M.J., Robinson, C.T., Schleiss, A.J., 2020. Erosion, transport and deposition of a sediment replenishment under flood conditions. Earth Surf. Process. Landforms. 45, 3354–3367.

Vercruysse, K., Grabowski, R.C., Rickson, R.J., 2017. Suspended sediment transport dynamics in rivers: Multi-scale drivers of temporal variation. Earth Sci. Rev. 166, 38–52.

Vaughan, M.C.H., Bowden, W.B., Shanley, J.B., Vermilyea, A., Sleeper, R., Gold, A.J., Pradhanang, S.M., Inamdar, S.P., Levia, D.F., Andres, A.S., Birgand, F., Schroth, A. W., 2017. High-frequency dissolved organic carbon and nitrate measurements reveal differences in storm hysteresis and loading in relation to land cover and seasonality. Wat. Resour. Res. 53 (7), 5345–5363.

Williams, G.P., 1989. Sediment concentration versus water discharge during single hydrologic events in rivers. J. Hydrol. 111 (1-4), 89–106.

Zhang, J., Shang, Y., Liu, J., Fu, J., Wei, S., Tong, L., 2020. Causes of variations in sediment yield in the Jinghe River Basin. China. Sci. Rep. 10 (1).